

SUPPORTING INFORMATION

Bond Dissociation Energies of Low-Valent Lanthanide Hydroxides: Lower Limits from Ion-Molecule Reactions and Comparisons with Fluorides

Mariah L. Parker, Jiwen Jian, and John K. Gibson

Chemical Sciences Division, Lawrence Berkeley National Laboratory, Berkeley, CA 94720
USA

Contents

Table S1. Summary of reported reactions of lanthanide cations with hydroxide donors.

Table S2. Summary of previously reported reactions of lanthanide cations with halide donors.

Table S3. Assessed and computed *BDEs* for lanthanide diatomics.

Table S4. Selected differences between *BDEs* in Table S3.

Figure S1. Representative ESI mass spectra of LnCl_3 solutions ($\text{Ln} = \text{Eu}, \text{Tm}, \text{Yb}$).

Figure S2. Kinetics results for reaction (3'): $\text{Ln}^+ + \text{H}_2\text{O} \rightarrow \text{LnOH}^+ + \text{H}$ ($\text{Ln} = \text{Eu}, \text{Tm}, \text{Yb}$)

Figure S3. Mass spectrum for hydration of $\text{UO}_2(\text{OH})^+$ used to calibrate $\text{P}[\text{H}_2\text{O}]$.

Figure S4. Reaction (3') kinetics plots for ion isolation widths $\Delta m/z$ of 1.0 and 2.0.

Figure S5. Reaction (3') kinetics for background water and with added water.

Figure S6. Differences between reported lanthanide fluoride and chloride *BDEs*.

Figure S7. Procedure and results for estimation of fully ionic *BDEs*.

Table S1. Results for reaction (3) with an OH-donor alcohol, and (3') with OH-donor water.^a

Ln⁺	R=H^b <i>BDE=498.8</i>	R=C₆H₅^c <i>BDE=474±8</i>	R=CH₃^c <i>BDE=390±10</i>	R=CH₃CH₂^c <i>BDE=392±4</i>	R=(CH₃)₂CH^c <i>BDE=402±2</i>
La ⁺	Yes	No/Other	Yes	Yes	Yes
Ce ⁺	No/Other	No/Other	Yes	Yes	Yes
Pr ⁺	Yes	No/Other	Yes	Yes	Yes
Nd ⁺	No/Other	Yes	Yes	Yes	Yes
Pm ⁺	NS	NS	NS	NS	NS
Sm ⁺	No/Other	Yes	Yes	Yes	Yes
Eu⁺	Yes^d	Yes	Yes	Yes	Yes
Gd ⁺	No/Other	No/Other	Yes	Yes	Yes
Tb ⁺	No/Other	No/Other	Yes	Yes	Yes^f
Dy ⁺	No	No/Other	No/Other	Yes	Yes
Ho ⁺	No	No/Other	No/Other	Yes	No/Other
Er ⁺	No	No/Other	No/Other	Yes	No/Other
Tm⁺	Yes^d	No/Other	No	No	No
Yb⁺	Yes^e	No	No	No	No
Lu ⁺	No/Other	No/Other	Yes	Yes	Yes

^a Results are for OH-abstraction: Yes = Observed; No = Not observed; No/Other = Possibly obscured by another reaction; NS = Not Studied. Red = also studied in the present work. Abstraction under thermal conditions indicates $BDE[Ln^+-OH] \geq BDE[R-OH]$ (given in kJ/mol¹).

^bSIFT results from Bohme, et al.²

^cICR results from Marçalo, et al.^{3,4} The reactant alcohols are phenol methanol, ethanol and isopropanol.

^dQIT results from this work; reaction not seen by SIFT.²

^eConfirmed in the present work by QIT.

Table S2. Reported reactions of lanthanide cations with halide donors.^{a,b}

Ln⁺	CH₃F	SF₆	C₆H₅F	CH₃Cl	C₆H₅Cl
La ⁺	✓	✓	✓	✓	✓
Ce ⁺	✓	✓	✓	✓	✓
Pr ⁺	✓	✓	✓	✓	✓
Nd ⁺	✓	✓	✓	✓	✓
Pm ⁺	-	-	-	-	-
Sm ⁺	✓	✓	✓	✓	✓
Eu ⁺	✓	✓	✓	✓	✓
Gd ⁺	✓	✓	✓	✓	✓
Tb ⁺	✓	✓	✓	✓	✓
Dy ⁺	✓	✓	✓	✓	✓
Ho ⁺	✓	✓	✓	✓	✓
Er ⁺	✓	✓	✓	✓	✓
Tm ⁺	✓ ^c	✓	✓	✓ ^d	✓
Yb ⁺	✓ ^c	✓	✓	✓ ^d	✓
Lu ⁺	✓	✓	✓	✓	✓
<i>BDE</i>[Ln⁺-X]^e	≥ 459±1	≥ 392±1	≥ 534±9	≥ 351±1	≥ 406±8

^aA check mark (✓) indicates that abstraction of a halogen atom X from the donor RX to yield LnX⁺ was observed; a dash (-) indicates that the reaction was not studied.

^bResults are from: Ref.⁵ for SF₆; Ref.⁶ for CH₃F; Ref.⁷ for CH₃Cl; Ref.⁸ for C₆H₅Cl and C₆H₅F.

^cAlso studied by Cornehl et al. using FTICR-MS, with no reaction reported.⁹

^dProduct reported in Ref.⁷ with only an upper limit given for the reaction rate.

^eLower limit for *BDE*[Ln⁺-X] (kJ/mol) indicated for those Ln⁺ that exhibit abstraction. *BDEs* for donors are from NIST Chemistry WebBook.¹

Table S3. Assessed and computed *BDEs* (kJ/mol) for lanthanide diatomics.

	(1)	(1')	(2)	(3)	(4)	(5)	(6)	(7)	(8)
<i>Ln</i>	<i>Ln⁺-F^a</i> <i>C&C</i> <i>Pref.</i>	<i>Ln⁺-F^a</i> <i>C&C</i> <i>Alt.</i>	<i>Ln⁺-Cl^a</i> <i>C&C</i>	<i>Ln⁺-F^b</i> <i>KHF</i>	<i>Ln⁺-Cl^b</i> <i>KHF</i>	<i>Ln-F^a</i> <i>C&C</i>	<i>Ln-Cl^a</i> <i>C&C</i>	<i>Ln-OH^c</i> <i>Comp.</i>	<i>Ln-F^d</i> <i>Comp.</i>
<i>La</i>	695	656	529	659	504	644	500	560	672
<i>Ce</i>	678	630	512	612	429	626	490	553	665
<i>Pr</i>	669		493	611	445	604	470	481	589
<i>Nd</i>	639		471	602	441	580	448	445	567
<i>Pm^e</i>	623		459	601	435	566	436	452	569
<i>Sm</i>	609		455	607	435	556	431	437	528
<i>Eu</i>	594		442	584	431	550	419	426	554
<i>Gd</i>	671	614	491	589	404	615	467	531	596
<i>Tb</i>	648	579	476	621	417	604	457	679	794
<i>Dy</i>	584		436	535	408	547	412	577	567
<i>Ho</i>	596	558	435	513	410	558	418	586	698
<i>Er</i>	598	555	440	549	407	574	429	500	527
<i>Tm</i>	545		409	537	408	515	384	369	503
<i>Yb</i>	519		387	557	400	486	361	389	513
<i>Lu</i>	586	481	446	377	181	623	462	624	740

^aFrom *C&C*:¹⁰ *Preferred* (1) and *Alternate* (1') for LnF^+ from Table 6; the two sets were obtained from $BDE[\text{Ln-F}]$ using different values for $IE[\text{LnF}]$; (2) LnCl^+ from Table 6; (5) LnF from Table 4 recommended values; (6) LnCl from Table 3 third law values (other values there are similar).

^bFrom *KHF* Table 5:¹¹ (3) and (4).

^cFrom Dixon et al., 2017¹²: Table 7, reaction (3) R/UCCSD(T), and $BDE[\text{HO-OH}] = 214.1$ kJ/mol.¹

^dFrom Dixon et al., 2011:¹³ Table 6, U/UCCSD(T), and $BDE[\text{CH}_3\text{-F}] = 459.4$ kJ/mol.¹

^eValues for Pm are purely estimates as there are no experimental data.

Table S4. Selected differences between *BDEs* in Table S3.

	(1)-(2) LnF ⁺ -LnCl ⁺ <i>C&C Pref.</i>	(1')-(2) LnF ⁺ -LnCl ⁺ <i>C&C Alt.</i>	(3)-(4) LnF ⁺ -LnCl ⁺ <i>KHF</i>	(5)-(6) LnF-LnCl <i>C&C</i>	(8)-(7) LnF-LnOH <i>Computed</i>	(1)-(5) LnF ⁺ -LnF <i>C&C</i>
<i>La</i>	166	127	155	144	112	51
<i>Ce</i>	166	118	183	136	112	52
<i>Pr</i>	176		166	134	108	65
<i>Nd</i>	168		161	132	122	59
<i>Pm</i>	164		166	130	117	57
<i>Sm</i>	154		172	125	91	53
<i>Eu</i>	152		153	131	128	44
<i>Gd</i>	180	123	185	148	65	56
<i>Tb</i>	172	103	204	147	115	44
<i>Dy</i>	148		127	135	-10	37
<i>Ho</i>	161	123	103	140	112	38
<i>Er</i>	158	115	142	145	27	24
<i>Tm</i>	136		129	131	134	30
<i>Yb</i>	132		157	125	124	33
<i>Lu</i>	140	35	196	161	116	-37

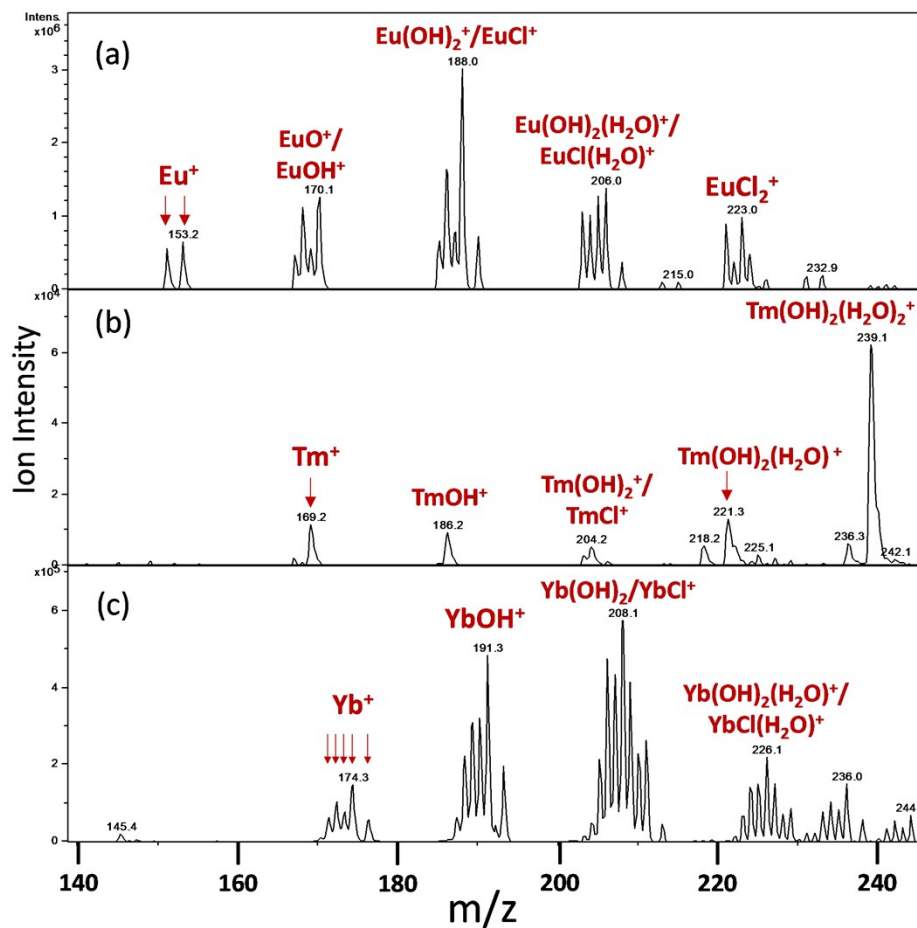


Figure S1. Representative ESI mass spectra for solutions of (a) EuCl_3 ; (b) TmCl_3 ; (c) YbCl_3 , acquired before isolation of one isotope of bare Ln^+ for reactivity studies. Relative abundances of the various species can vary substantially upon changing experimental parameters such as the ESI and ion transfer voltages, and the ion trap drive. In contrast to products of ion-molecule reactions in the QIT, the species in these spectra were produced either during the ESI process or subsequently as a result of reactions during substantially hyperthermal ion transport from the ESI source to the ion trap.

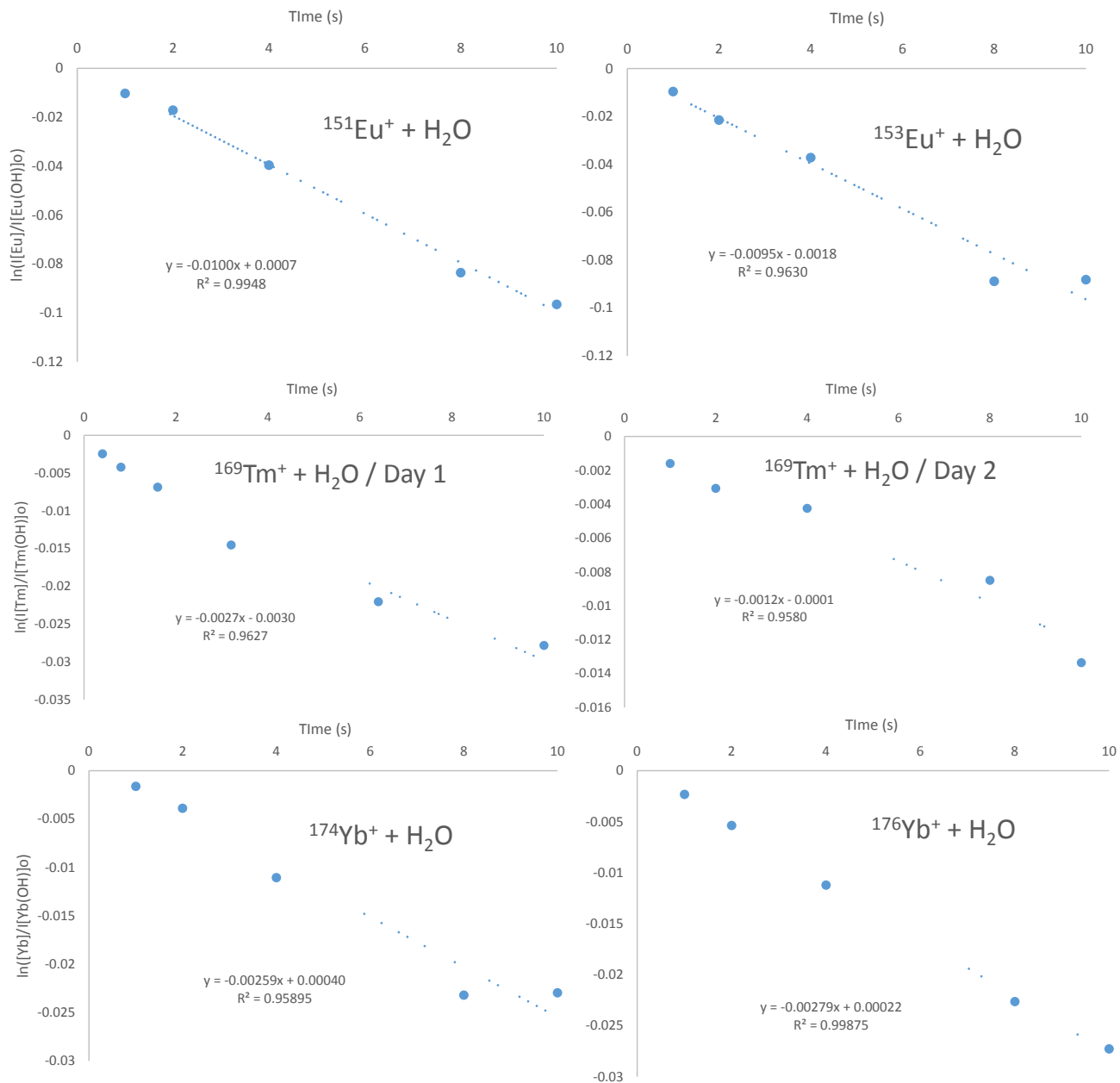


Figure S2. Kinetics results for reaction (3') using the background water in the ion trap. Top: Two isotopes of Eu^+ . Middle: $^{169}\text{Tm}^+$ on two days with different water pressures. Bottom: Two isotopes of Yb^+ .

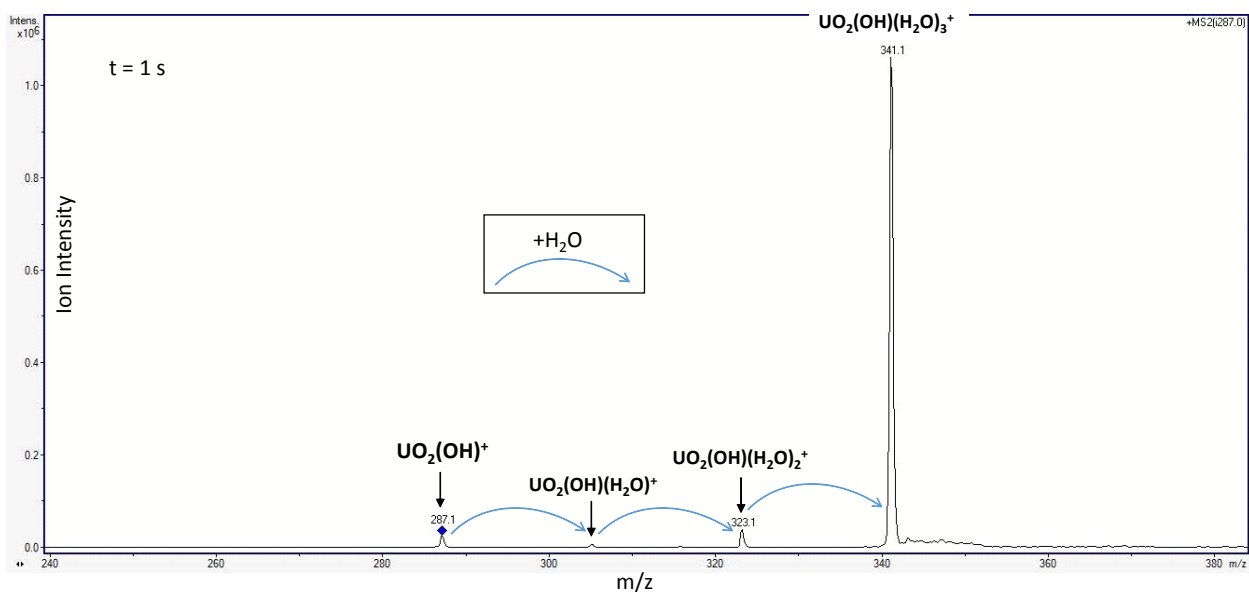


Figure S3. Mass spectrum acquired after isolation of $\text{UO}_2(\text{OH})^+$ at 287 m/z for 1 s. Hydration to the terminal trihydrate at 341 m/z is $>90\%$ complete after the reaction with background water for 1 s. The primary hydration step employed to calibrate the variable water pressure in the trap is much faster than reaction (3') for the bare Ln^+ .

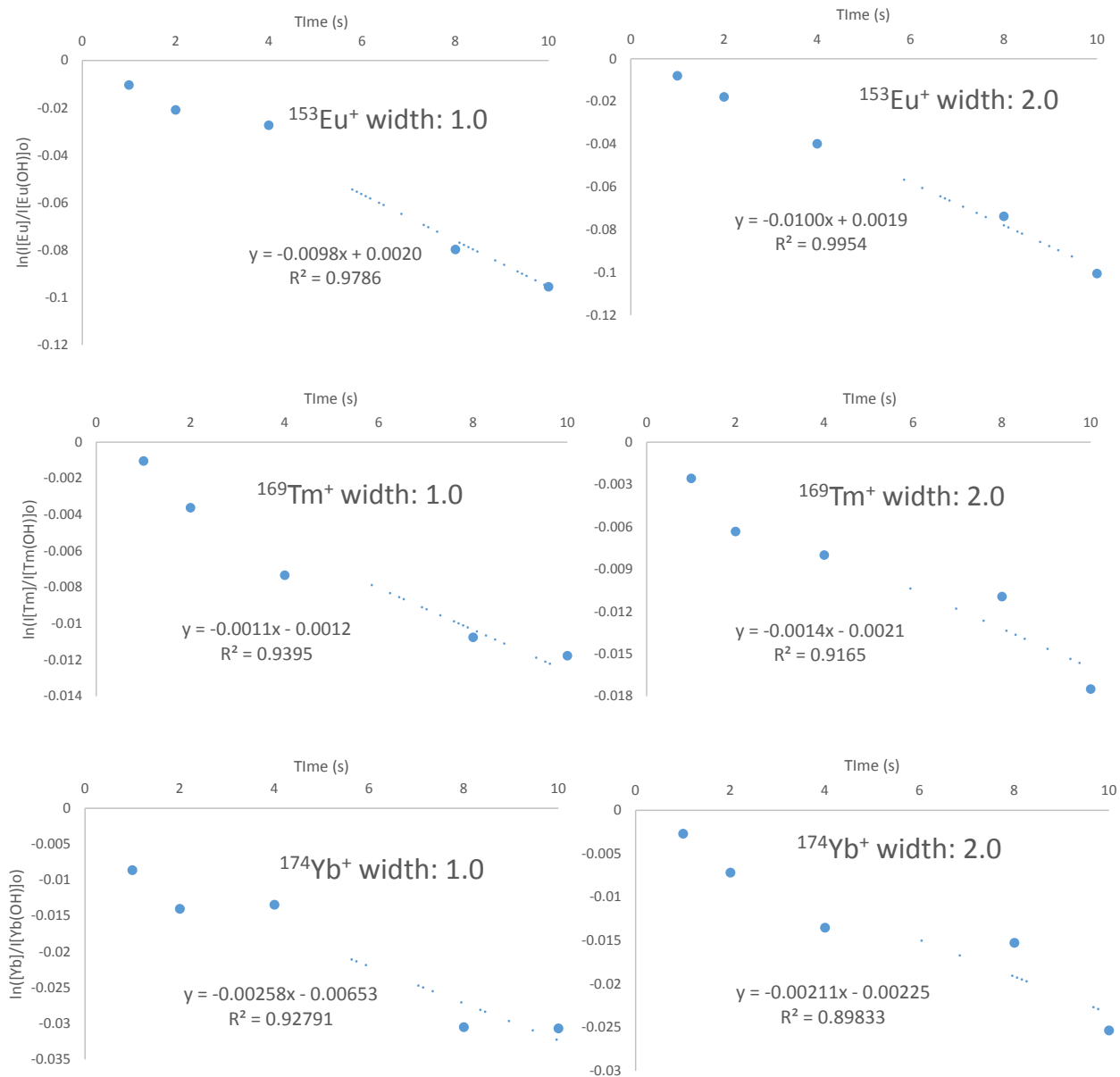


Figure S4. Reaction (3') kinetics plots acquired for ion isolation widths ($\Delta m/z$) of 1.0 and 2.0. The fitted slopes indicate essentially the same kinetics for the two isolation widths, and thus negligible effects of off-resonance ion excitation.

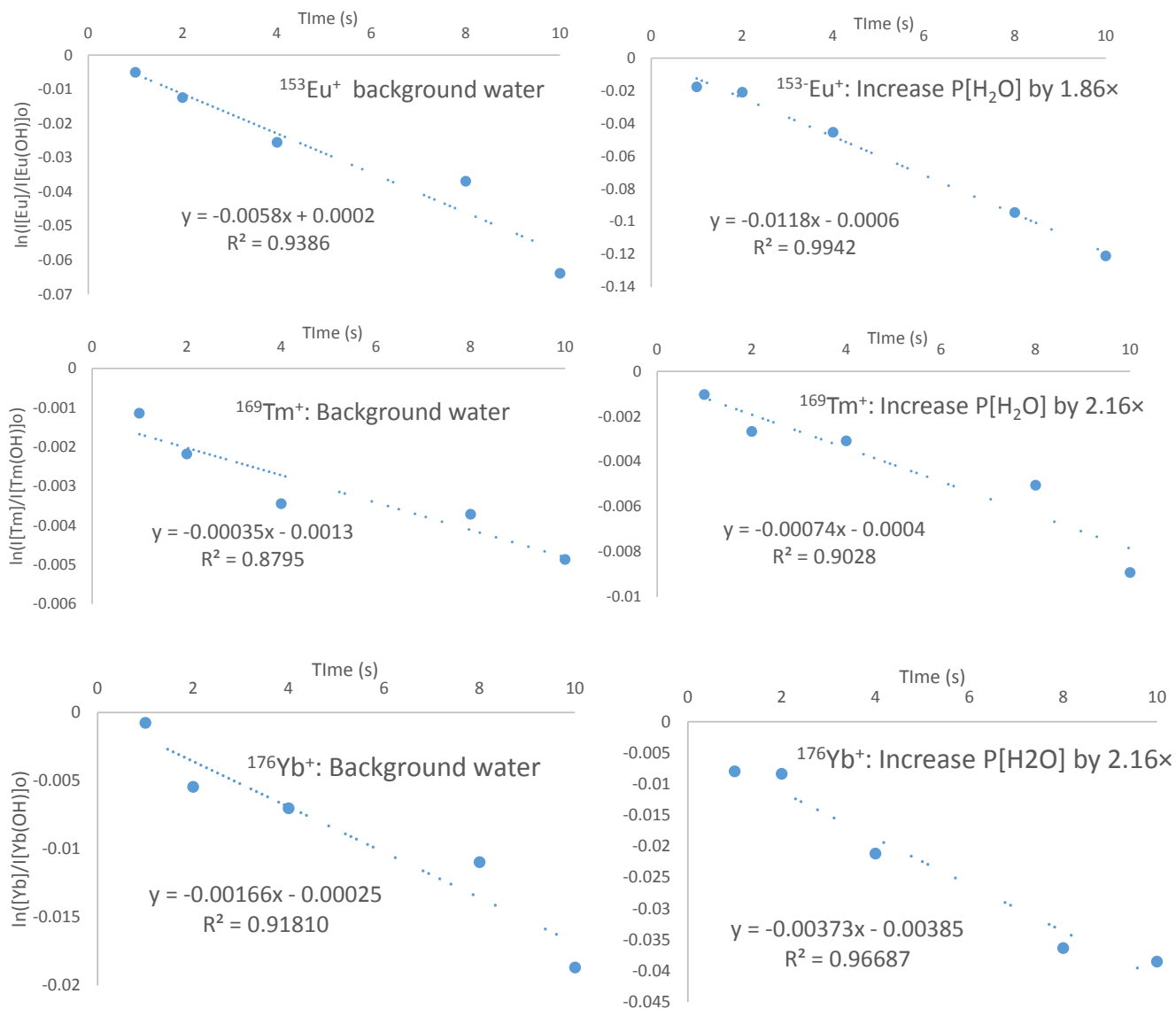


Figure S5. Reaction (3') kinetics plots acquired using only background water in the ion trap (plots on left hand side), and after increasing the water pressure by the indicated factor (plots on right hand side; the $P[\text{H}_2\text{O}]$ was increased by a factor of $\sim 2\times$). The reaction rates increase as expected with increasing water pressure, confirming reaction (3').

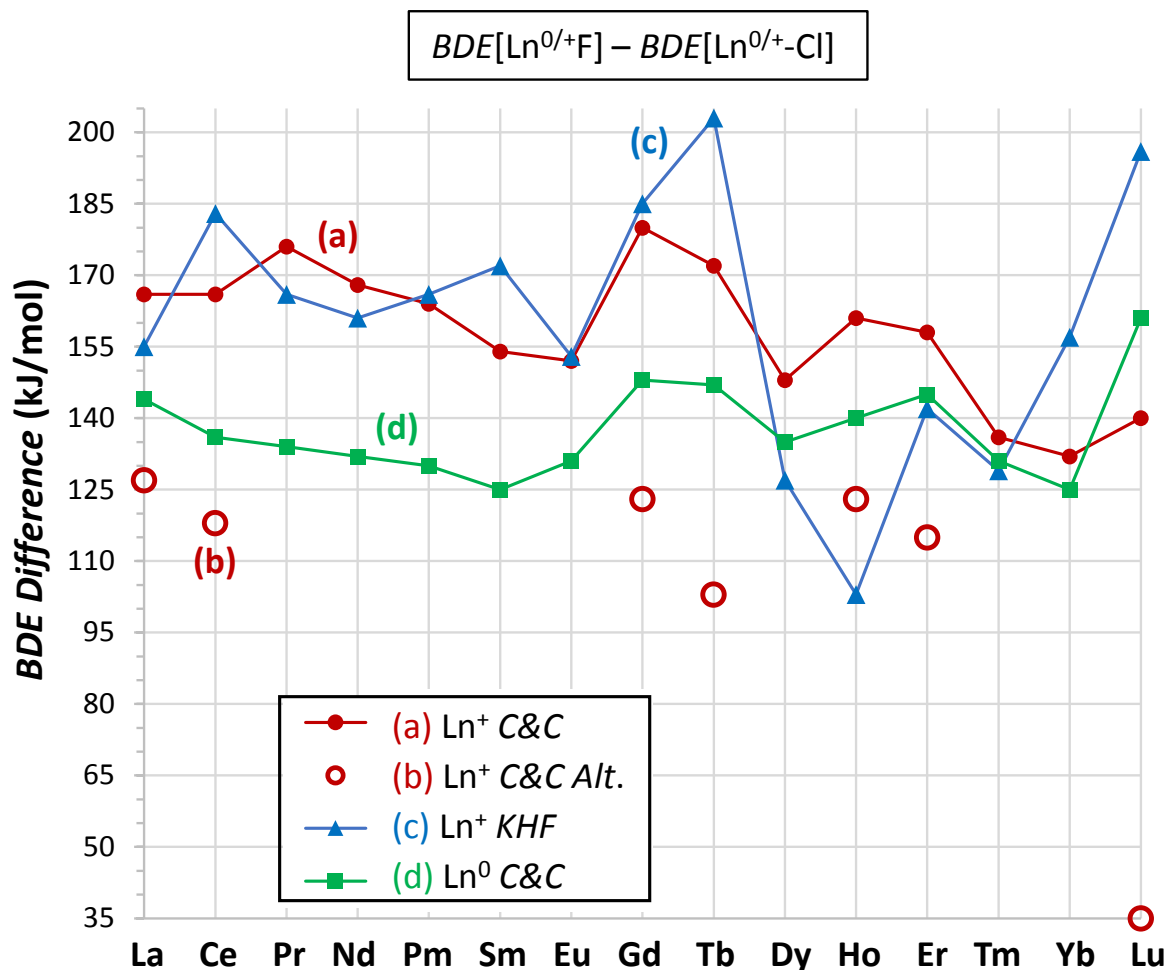
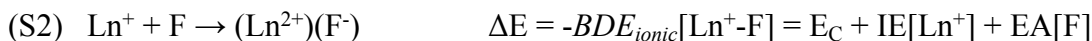
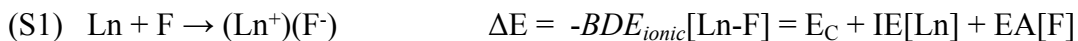


Figure S6. Difference between fluoride and chloride bond energies: $BDE[\text{Ln}^{0/+}\text{-F}] - BDE[\text{Ln}^{0/+}\text{-Cl}]$ (differences in Table S3). (a) Solid red circles = cations LnX^+ , using *preferred* fluoride values from C&C [(1)-(2)]; (b) Open red circles = cations LnX^+ , using *alternate* fluoride values from C&C [(1')-(2)]; (c) Solid blue triangles = cations LnX^+ , using values from *KHF* [(3)-(4)]; (d) Solid green squares = neutrals LnX , using values from C&C.

As the bonding of lanthanides to fluorides and chlorides is presumed to be essentially of a comparable nature, the difference between fluoride and chloride *BDEs* is expected to be similar across the lanthanide series. For the neutral lanthanides ((d)/green squares) the difference $BDE[\text{Ln-F}] - BDE[\text{Ln-Cl}]$ falls in the fairly narrow range of 125-148 kJ/mol, except for the larger difference of 161 kJ/mol for Lu. Variations in the cation lanthanide difference $BDE[\text{Ln}^+\text{-F}] - BDE[\text{Ln}^+\text{-Cl}]$ are larger than for neutrals. The cation difference is in the range of 132-180 kJ/mol using the *preferred* values from C&C ((a)/solid red circles). This range increases to 103-180 kJ/mol for the *alternate* values from C&C, excluding the very small difference of only 35 kJ/mol for Lu ((b)/open red circles). The cation difference using the *KHF* values ranges from 103-203 kJ/mol, with particularly large deviations for Tb, Ho and Lu. The smaller variation in $BDE[\text{Ln}^+\text{-F}] - BDE[\text{Ln}^+\text{-Cl}]$ for the *preferred* C&C values (closed circles) versus *alternate* C&C values (open circles) is a primary criterion for assignment of values as “preferred”.

Estimation of hypothetical fully ionic BDE_{ionic}

An informative extreme model is that of fully ionic bonding. The goal here of considering such a model is not to accurately predict $BDEs$ but rather to compare expected trends for such bonding with actual $BDEs$. In the ionic limit, neutral fluoride LnF is represented as $(Ln^+)(F^-)$ and cation LnF^+ as $(Ln^{2+})(F^-)$, as in reactions (S1) and (S2), respectively. The cation-anion interaction energy is given by the Coulomb equation: $E_C = -[1389.4 \text{ (kJ/mol)}(\text{\AA})/(\text{e})^2][q_1q_2/r]$ where q_1 and q_2 are the charges on the two ions, and r is the distance between them. In addition to the energy gained by the Coulomb interaction, other components of fully ionic BDE_{ionic} are the ionization energy (IE) to create the cation and the electron affinity (EA), which is the energy gained in creating the anion; IE is defined as a positive quantity whereas EA is (usually) negative. To obtain E_C for LnF , $(Ln^+)(F^-)$, and LnF^+ , $(Ln^{2+})(F^-)$, we employ $IE[Ln^+]$ and $IE[Ln^{2+}]$ values from NIST,¹⁴ and interatomic distances r derived as follows. A simple linear interpolation between computed distances for LaF ($r = 2.02 \text{ \AA}$) and LuF ($r = 1.92 \text{ \AA}$) was employed to obtain distances for the other LnF containing intermediate lanthanides between La and Lu .¹⁵ The distances for LnF^+ were then obtained from those for LnF by applying to all of the neutral distances the same 0.05 \AA contraction that was computed for DyF^+ versus DyF .¹⁶ Without suggesting validity of the obtained absolute values for BDE_{ionic} , the results in Figure S7 demonstrate regular variations in E_C due to decreasing interatomic distance with increasing nuclear charge across the series. A key result is that the predicted variations in E_C are small relative to differences in ionization energies, such that the latter dominate variations in BDE_{ionic} .



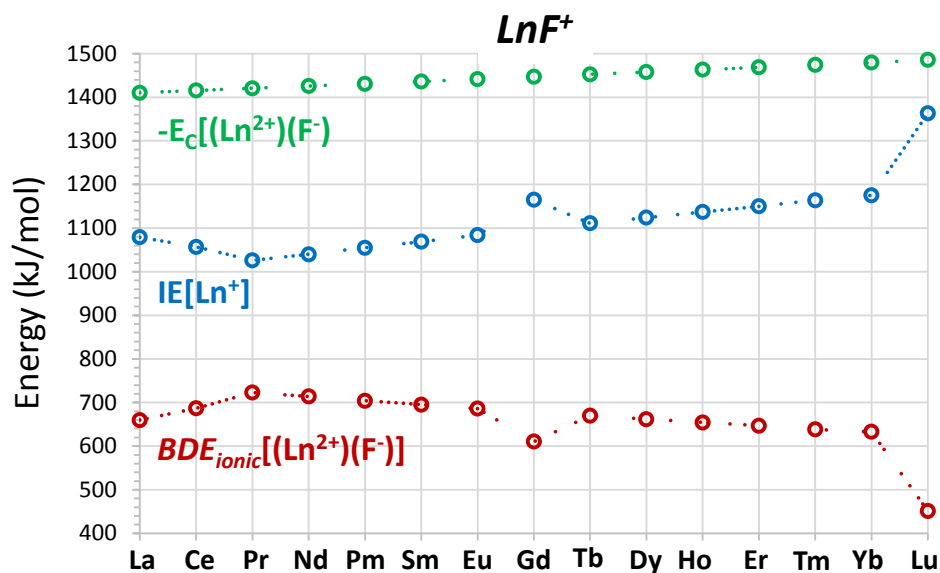
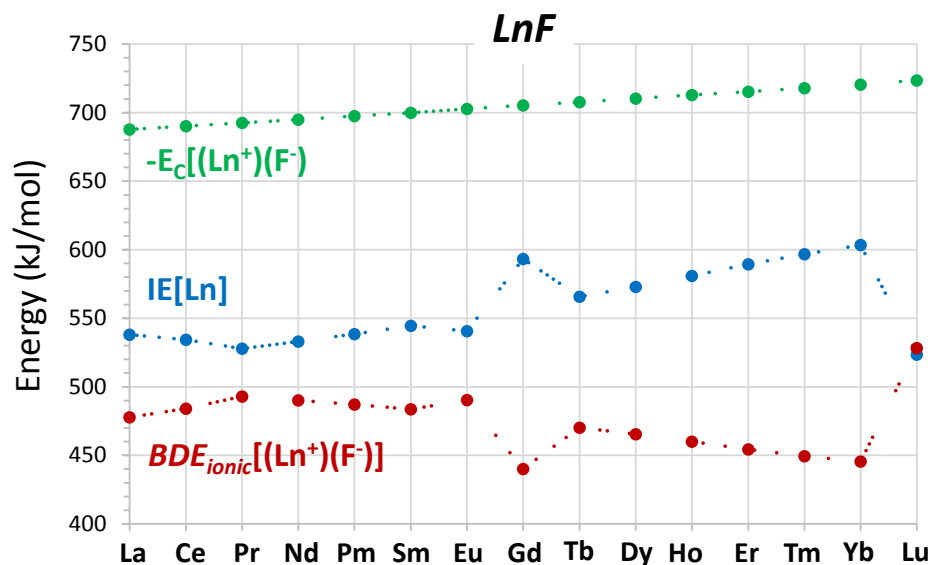


Figure S7. Dissociation energies BDE_{ionic} for LnF (in the top plots, red points) and LnF^+ (in the bottom plots, red points) obtained from the simple model of fully ionic bonding. Constituent ionization energies (IE, blue points) and Coulomb energies (E_C , green points) are also shown. The variations in E_C are much smaller and more regular than for the IEs, such that the variations in BDE_{ionic} primarily reflect those in IEs. Both $IE[Lu]$ and $IE[Lu^+]$, and the resulting BDE_{ionic} for LuF and LuF^+ are characteristically deviant. There are smaller but significant deviations for Gd.

References

1. Linstrom, P. J., NIST Chemistry WebBook, NIST Standard Reference Database Number 69. National Institute of Standards and Technology: Gaithersburg, MD, USA, 2020.
2. Cheng, P.; Koyanagi, G. K.; Bohme, D. K., Gas-Phase Reactions of Atomic Lanthanide Cations with D₂O: Room-Temperature Kinetics and Periodicity in Reactivity. *ChemPhysChem* **2006**, *7* (8), 1813-1819.
3. Carretas, J. M.; de Matos, A. P.; Marçalo, J.; Pissavini, M.; Decouzon, M.; Géribaldi, S., Gas-Phase Reactivity of Rare Earth Cations with Phenol: Competitive Activation of C-O, O-H, and C-H Bonds. *J Am Soc Mass Spectrom* **1998**, *9* (10), 1035-1042.
4. Carretas, J. A.; Marçalo, J.; de Matos, A. P., Gas-Phase Reactions of Lanthanide Cations with Alcohols. *Int J Mass Spectrom* **2004**, *234* (1-3), 51-61.
5. Cheng, P.; Bohme, D. K., Gas-Phase Reactions of Atomic Lanthanide Cations with Sulfur Hexafluoride: Periodicity in Reactivity. *Inorg Chem* **2006**, *45* (19), 7856-7863.
6. Zhao, X.; Koyanagi, G. K.; Bohme, D. K., Gas-Phase Reactions of Atomic Lanthanide Cations with Methyl Chloride - Periodicities in Reactivity. *Can J Chem* **2005**, *83* (11), 1839-1846.
7. Koyanagi, G. K.; Zhao, X.; Blagojevic, V.; Jarvis, M. J. Y.; Bohme, D. K., Gas-Phase Reactions of Atomic Lanthanide Cations with Methyl Fluoride: Periodicities Reactivity. *Int J Mass Spectrom* **2005**, *241* (2-3), 189-196.
8. Zhou, S. D.; Schlangen, M.; Schwarz, H., Mechanistic Aspects of the Gas-Phase Reactions of Halobenzenes with Bare Lanthanide Cations: A Combined Experimental/Theoretical Investigation. *Chem-Eur J* **2015**, *21* (5), 2123-2131.
9. Cornehl, H. H.; Hornung, G.; Schwarz, H., Gas-Phase Reactivity of Lanthanide Cations with Fluorocarbons: C-F versus C-H and C-C Bond Activation. *J Am Chem Soc* **1996**, *118* (41), 9960-9965.
10. Chervonnyi, A. D.; Chervonnaya, N. A., Thermodynamic Properties of Lanthanum and Lanthanide Halides: IV. Enthalpies of Atomization of LnCl, LnCl⁺, LnF, LnF⁺, and LnF₂. *Russ J Inorg Chem* **2007**, *52* (12), 1937-1952.
11. Kaledin, L. A.; Heaven, M. C.; Field, R. W., Thermochemical Properties (D⁰ and IP) of the Lanthanide Monohalides. *J Mol Spectrosc* **1999**, *193* (2), 285-292.
12. Wang, X. F.; Andrews, L.; Fang, Z. T.; Thanthiriwatte, K. S.; Chen, M. Y.; Dixon, D. A., Properties of Lanthanide Hydroxide Molecules Produced in Reactions of Lanthanide Atoms with H₂O₂ and H₂ + O₂ Mixtures: Roles of the plus I, plus II, plus III, and plus IV Oxidation States. *J Phys Chem A* **2017**, *121* (8), 1780-1797.
13. Chen, M. Y.; Dixon, D. A.; Wang, X. F.; Cho, H. G.; Andrews, L., Matrix Infrared Spectroscopic and Electronic Structure Investigations of the Lanthanide Metal Atom-Methyl Fluoride Reaction Products CH₃-LnF and CH₂-LnHF: The Formation of Single Carbon-Lanthanide Metal Bonds. *J Phys Chem A* **2011**, *115* (22), 5609-5624.
14. Kramida, A.; Ralchenko, Y.; Reader, J., NIST Atomic Spectra Database, NIST Standard Reference Database 78. 2019 ed.; National Institute of Standards and Technology (NIST): Gaithersburg, MD, USA, 2019.
15. Solomonik, V. G.; Smirnov, A. N., Toward Chemical Accuracy in ab Initio Thermochemistry and Spectroscopy of Lanthanide Compounds: Assessing Core-Valence Correlation, Second-Order Spin-Orbit Coupling, and Higher Order Effects in Lanthanide Diatomics. *J Chem Theory Comput* **2017**, *13* (11), 5240-5254.
16. Saloni, J.; Roszak, S.; Hilpert, K.; Miller, M.; Leszczynski, J., Quantum Chemical Studies of Neutral, and Ionized DyX, DyX₂, and DyX₃ Species (X = F, Cl, Br, I) and the Implications for the Mass Spectra of Gaseous DyX₃. *Eur J Inorg Chem* **2004**, (6), 1212-1218.